Multiple Auger decay probabilities of neon from the 1*s*-core-hole state

Yulong Ma,[1] Fuyang Zhou,[2] Ling Liu,[2] and Yizhi Qu[1,*]

[1]*College of Material Sciences and Optoelectronic Technology, University of Chinese Academy of Sciences, Beijing 100049, China*

[2]*Data Center for High Energy Density Physics, Institute of Applied Physics and Computational Mathematics, Beijing 100088, China*

(Received 24 July 2017; published 19 October 2017)

The multiple Auger decays of the Ne $1s^{-1}$ state including double and triple Auger processes are investigated within the framework of perturbation theory. The contributions of the cascade and direct processes are determined for the double Auger decay. In the cascade processes, the choice of the orbital sets and configuration interaction can strongly affect the partial probabilities for the specific configurations of Ne^{3+}. The multistep approaches, i.e., the knockout and shakeoff mechanisms, are implemented to deal with the direct double Auger processes for which the total and partial probabilities corresponding to specific configurations of Ne^{3+} are calculated and reveal that the knockout is dominant. Finally, the probabilities of the triple Auger decays that are decomposed into a double Auger process and a subsequent emission of a single electron are obtained using the cascade and knockout mechanisms. The calculated probabilities agree reasonably well with the available experimental data.

DOI: 10.1103/PhysRevA.96.042504

I. INTRODUCTION

Auger decay is one of the relaxation processes of atoms and ions with an inner-shell vacancy during which one of the outer-shell electrons is emitted when a vacancy is filled by another outer-shell electron. It is known that a multiple Auger decay with ejection of two or more electrons constitutes a sizable fraction in the total Auger intensity. As a high-order process, the multiple Auger transitions provide valuable information on electron correlations and, more generally, many-body problems in atomic processes [1,2]. Besides, investigations of Auger decays are of great interest to various application fields, such as plasma physics [3,4], astrophysics [5,6], and x-ray laser schemes [7,8].

The double Auger (DA) decay was discovered by Carlson and Krause [9] by detecting the yields of Ne^{3+} formed in the Ne $1s^{-1}$ DA decay. Generally, the produced higher-charge ion's fraction in total decay is considered to be the probability (in percentages) for the multiple Auger decay [9]. Later experiments more accurately determined the fraction (∼6.0%) of the contribution for the DA decay and (∼0.3%) for the triple Auger (TA) decay, respectively, of the Ne $1s^{-1}$ state [10,11]. The emission of two electrons in the DA decay can be simultaneous, or it can proceed in a stepwise manner through the creation and decay of an intermediate Ne^{2+} state, which are referred to as the direct and cascade DA processes, respectively. By using multielectron coincidence spectroscopy, Hikosaka *et al.* [12] clarified the contributions from the direct and cascade DA processes according to the different ways in energy sharing between the two Auger electrons, and the partial probabilities for the specific electronic configurations of the final ion were obtained.

Many theoretical efforts have been made to interpret the DA decays of the Ne $1s^{-1}$ state. The theoretical results considering only the shakeoff (SO) mechanism yield apparently smaller fractions 0.5% [9] and 0.7% [13] for the Ne $1s^{-1}$ DA decay against the experimental values of about 6%. Amusia *et al.* [14] improved calculations including knockout (KO), SO, and cascade mechanisms to determine the DA probabilities within the many-body perturbation theory (MBPT). However, the calculated DA probability of 1.5% for the transition $1s^{-1} \rightarrow 2s^{-2}2p^{-1}$ and the estimated total DA probability of 4% are still smaller than the experimental results. The study by Kochur *et al.* [15] considering the final-state correlation of core electrons and core electrons with Auger electrons resulted in the DA probability of 5.39%, which is in the best agreement with the measurements. Therefore, considerations of both the correlation of the core electrons and the correlation of the core and Auger electrons (inelastic scattering by core electrons) are pivotal for the theoretical analysis of the DA decay in the Ne $1s^{-1}$ state.

In this paper we investigate the multiple Auger decays including the DA and TA processes for the Ne $1s^{-1}$ state using the multistep approaches derived from MBPT, namely, cascade, knockout, and shakeoff mechanisms. The probabilities of the cascade and direct DA processes are obtained that are reasonably consistent with experimental values. The influences of the orbital sets of the intermediate Ne^{2+} states and configuration interaction (CI) on the cascade DA probabilities are explored as well.

II. THEORY

The Ne $1s^{-1}$ state lies above the ground configurations of Ne^{2+}, Ne^{3+}, and Ne^{4+}, which can decay via single Auger (SA), DA, and TA transitions, schematically represented as follows:

$$\text{Ne } 1s^{-1}(\alpha) \xrightarrow{\text{Auger}} \text{Ne}^{2+}(\beta) + e^-(\varepsilon l), \tag{1}$$

$$\text{Ne } 1s^{-1}(\alpha) \xrightarrow{\text{double Auger}} \text{Ne}^{3+}(\gamma) + e^-(\varepsilon_1 l_1) + e^-(\varepsilon_2 l_2), \tag{2}$$

$$\text{Ne } 1s^{-1}(\alpha) \xrightarrow{\text{triple Auger}} \text{Ne}^{4+}(\delta) + e^-(\varepsilon_1 l_1) + e^-(\varepsilon_2 l_2) + e^-(\varepsilon_3 l_3). \tag{3}$$

The SA decay rate can be obtained by [16,17]

$$A^1_{\alpha\beta} = \left| \langle \psi^+_\beta, \kappa; J_T M_T | \sum_{i<j}^{N} \frac{1}{r_{ij}} | \psi_\alpha \rangle \right|^2, \tag{4}$$

where ψ_α represents the initial autoionizing state wave function with N electrons and $|\psi^+_\beta, \kappa; J_T M_T\rangle$ is the final

*yzqu@ucas.ac.cn

ionic state $|\psi_\beta^+\rangle$ with $N-1$ electrons plus a continuum Auger electron with the relativistic angular quantum number κ. J_T is the total angular momentum of the final ionic state coupling with the continuum Auger electron, and M_T is the magnetic quantum number of the total angular momentum.

Since the matrix element $\langle\psi_\gamma^{2+},\kappa_1,\kappa_2; J_T M_T|\sum_{i<j}^{N}\frac{1}{r_{ij}}|\psi_\alpha\rangle$ involving the change in more than two single-electron orbitals between the initial and the final wave functions vanishes, the independent-particle model fails to determine the amplitude of the multiple Auger processes. We employ the approximate formulas of direct (knockout and shakeoff) and cascade mechanisms to simplify the calculations of the DA rates [14,18–21].

The KO process could be considered as an impact ionization process [22]. The direct DA rate for the KO mechanism can be given by

$$A_{\mathrm{KO}}^2 = \sum_\beta A_{\alpha\beta}^1 \Omega_{\beta\gamma}(\varepsilon_0), \tag{5}$$

where $A_{\alpha\beta}^1$ is the SA rate from the initial-state α to the intermediate-state β and $\Omega_{\beta\gamma}(\varepsilon_0)$ is the collision strength of the inelastic scattering by the intermediate free electron with energy ε_0 from the SA process.

In contrast to the KO mechanism, the SO is a pure quantum effect in which the second Auger electron is ejected due to relaxation following a sudden change in the atomic potential caused by a rapid ejection of the first Auger electron. The direct DA rate of the SO mechanism can be expressed by

$$A_{\mathrm{SO}}^2 = \sum_\beta A_{\alpha\beta}^1 \left|\langle\psi_\gamma^{2+}\kappa; J_T M_T|\psi_\beta^+\rangle\right|^2, \tag{6}$$

where the matrix element $\langle\psi_\gamma^{2+}\kappa; J_T M_T|\psi_\beta^+\rangle$ represents the overlap integral between the intermediate-state β and the final-state γ with the second Auger electron being emitted. For high energies, the Auger electron interacts with an ion so quickly that the contribution of the KO mechanism drops and the main contribution is a SO mechanism [22].

In addition to the direct DA process, the DA process also includes the cascade process in which the initial autoionizing state can have a single Auger decay to an intermediate state that is embedded energetically within the continuum of the next-higher-charge state of the ion. Such an intermediate state can decay via another single Auger transition. The corresponding cascade DA rate can be obtained from the expression,

$$A_{\mathrm{CS}}^2 = \sum_\beta A_{\alpha\beta}^1 A_{\beta\gamma}^1 \Gamma_\beta^{-1}, \tag{7}$$

where $A_{\beta\gamma}^1$ is the single Auger rate from the intermediate resonance state β to the final-state γ and Γ_β is the total width of the intermediate-state β.

III. RESULTS AND DISCUSSION

The SA decay rates were calculated with the XAUGER component of the RATIP package [17]. The XAUGER program supports the evaluation of the many-electron Auger amplitude with nonorthogonality between the orbitals of the initial and final wave functions, and for the details please refer to Refs. [17,23–25] and references therein. The one-electron spin orbitals of the initial and final wave functions were optimized separately with the GRASP program [26], based on the multiconfiguration Dirac-Fock (MCDF) method. The atomic state functions (ASFs) were obtained by diagonalizing the Hamiltonian matrix in the basis of the antisymmetric configuration state functions using the XRELCI component [27] of the RATIP package. The direct DA decays in this paper are decomposed into multistep processes based on the KO and SO mechanisms described by Eqs. (5) and (6), respectively, in Sec. II above. These procedures require evaluations of the collision strengths involving two continuum electrons and that of the overlap integrals between the intermediate and the final states. Therefore, the flexible atomic code [16] with some modifications [21] was utilized to calculate the overlap integrals and the collision ionization strengths based on the distorted-wave approximation.

A. Single Auger decay

The calculated SA decay rates of Ne $1s^{-1}$ are shown in Table I, which are crucial for the evaluation of the DA rates. The previous theoretical studies [28–30] on the SA rates of Ne $1s^{-1}$ only included the bound states $(2s2p)^{-2}$ of Ne^{2+} for *KLL* Auger transitions. In this paper, both the bound states and the resonance states of Ne^{2+} are included. The latter can autoionize further until bound (or stable) states are reached; this is called the cascade process.

Theoretical studies of the Ne *KLL* Auger transitions by Tulkki *et al.* [29] with the relativistic multichannel MCDF method and by Yarzhemsky and Sgamellotti [30] with the MBPT method indicated that: (i) The choice of orbital sets of the initial state strongly affects the total SA rate, and (ii) the choice of the final orbital sets and different CI schemes result in redistribution of the SA rates to the final Ne^{2+} states, but the influences on the total SA rate are small. Here, we use three different models to explore the influences of the orbital sets of the final states and the CI effects on the SA rates of the Ne^{2+} states, especially the resonance states.

We solved the Dirac-Fock equations and carried out the self-consistency procedures for configurations $1s^2\,2s^2\,2p^4$, $1s^2\,2s2p^5$, and $1s^2\,2p^6$ to get the orbital set of the Ne^{2+} states for model I. Model II extended this approach by adding configuration $1s^2\,2s^2\,2p^3 3p$. The CI approximation was used in the calculations of the ASFs of the Ne^{2+} states with account of single and double excitations from the reference configurations $2s^2\,2p^4$, $2s2p^5$ to the active orbital space of nl ($n<4$, $l<3$) for models I and II. For model III, the orbital set was the same as in model II, but the active orbits extended up to $4l$ ($l<3$). The orbital set of Ne $1s^{-1}$ was constructed by the configuration $1s2s^2\,2p^6$ for three different models. The calculated total and partial SA rates in Table I show good agreement with the experimental results [31,32]. It is found that the total SA rate in model II is very close to that in model III, which means that the total SA rate converges with the orbital set of model II. The effect of the orbital set of Ne^{2+} on the partial SA rates decaying to bound states of the configurations $(2s2p)^{-2}$ in the Ne^{2+} ion is relatively small, but the partial SA rates decaying to resonance states in models II and III are about three times greater than the one in model I. It is found that the Ne $1s^{-1}$ state decays

TABLE I. Single Auger decay rates (10^{13} s^{-1}) for the main channels of Ne $1s^{-1}$ in models I–III. The numbers in square brackets represent powers of 10.

			Model			
Ne^{2+}	Term	J	I	II	III	Expt.
$2s^2\,2p^4$	^3P	2	3.86(−3)	4.11(−3)	3.96(−3)	
		1	1.09(−5)	1.02(−5)	1.00(−5)	
		0	4.26(−4)	4.49(−4)	4.25(−4)	
	^1D	2	23.45	22.17	22.07	24.56[a]
	^1S	0	2.80	2.61	2.57	3.88[a]
$2s2p^5$	^3P	2	1.82	1.64	1.64	
		1	1.07	0.97	0.97	2.58[a]
		0	0.36	0.32	0.32	
	^1P	1	8.60	7.13	7.25	7.04[a]
$2p^6$	^1S	0	2.35	2.45	2.52	2.54[a]
Resonance states			0.47	1.30	1.25	
Total			41.88	40.73	40.73	40.93 ±2.9[b]

[a]Reference [31].
[b]Reference [32].

preferentially into configurations $2s^2\,2p^4$, $2s2p^5$, and $2p^6$ of Ne^{2+} and the strongest transition is $2s^2\,2p^4\ ^1D_2$ with the rate of 2.21×10^{14} s^{-1} that accounts for 54% of the total SA rate, according to model III. The next strongest transition is $2s2p^5\ ^1P_1$ with a contribution of 18% to the total SA rate.

There are too many resonance states of Ne^{2+}, and we only present the summation of the rates of resonance states in Table I. These resonance states will further decay to Ne^{3+} states via a cascade DA process, which will be discussed in the next subsection.

B. Double Auger decay

1. The cascade double Auger process

To the best of our knowledge, there are very few theoretical studies of the cascade DA processes for the Ne $1s^{-1}$ state. We show the cascade DA probabilities (in percentages) in Table II based on models II and III, and the dominate channels originate from the configurations $2s^2\,2p^3$ and $2s2p^4$. The ratio of the partial cascade DA probabilities of these configurations is $(2s^2\,2p^3) : (2s2p^4) = 3.0 : 1$ for model II, whereas that from the experiment is 1.3:1 [12]. Since the resonance states included in the cascade processes are affected strongly by electron correlation, especially if several open shells are involved, in model III the larger-scale electron configuration space was included by extending the active orbits to $4l$ ($l < 3$) to explore the electron correlation effects on the partial cascade DA probabilities. The $4f$ orbital was not included in model III due to the computational challenge. However, it still took several weeks to calculate the SA rates for the decays of Ne $1s^{-1}$ to the fine-structure levels (with $J = 1$ only) of Ne^{2+} with the serial XAUGER program on a modern 2.40-GHz Intel Xeon-based cluster. In model III, the ratio of the partial cascade DA probabilities is improved to be $(2s^2\,2p^3) : (2s2p^4) = 1.7 : 1$. The high-$n$ ($n > 4$) Rydberg-excited resonance states in the intermediate Ne^{2+} ion cannot be included in this paper, but reasonable agreement between the theoretical and the experimental results for the total and partial cascade DA probabilities in model III is shown in Table II.

TABLE II. Probabilities (in percentages) of the cascade double Auger decays of Ne $1s^{-1}$ in models II and III.

	Model		
Ne^{3+}	II	III	Expt. [12]
$2s^2\,2p^3$	2.32	1.88	1.60
$2s2p^4$	0.78	1.09	1.20
Total	3.10	2.97	2.80

TABLE III. Probabilities (in percentages) of the direct double Auger decays of Ne $1s^{-1}$. The contributions from the knockout and shakeoff mechanisms are denoted by KO and SO, respectively. The calculated direct double Auger probabilities in column 4 with the inclusions of KO and SO are compared with experimental data [12].

Ne^{3+}	KO	SO	Direct DA	Expt. [12]
$2s^2\,2p^3$	1.14	0.16	1.30	0.90
$2s2p^4$	1.36	0.17	1.53	1.70
$2p^5$	0.30	0.04	0.34	0.50
Total	2.80	0.37	3.17	3.20

2. The direct double Auger process

Table III shows the direct DA probabilities (in percentages) including the KO and SO mechanisms as well as the measurements [12]. The calculated total direct DA probability of 3.17% is in good agreement with the experimental result of 3.20%. As observed by experiment, the strongest channel is to be configuration $2s2p^4$, which accounts for 48% of the total direct DA probability. The ratios of the partial direct DA probabilities of the configurations are $(2s^2\,2p^3) : (2s2p^4) : (2p^5) = 3.8 : 4.5 : 1$ from our results and 1.8:3.4:1 from the measurements thereby suggesting an overestimate of the contribution of $2s^2\,2p^3$ and an underestimate of $2s2p^4$ and $2p^5$ in our calculations. The contributions of the SO mechanism are smaller than those of the KO mechanism by an order of magnitude as shown in Table III, and the SO mechanism only yields the DA probability of 0.37% that is consistent with the previous calculations of 0.50% [9] and 0.70% [13]. Similar conclusions were reported for the direct DA processes of C^+ $1s^{-1}$ [21] and Ar $2p^{-1}$ [18], respectively. Schneider *et al.* [22] studied the double photoionization by a single photon based on the SO and KO mechanisms, which shows the SO mechanism is responsible in the high-energy limit, and hence the KO mechanism dominates for the Auger electron energies below 800 eV in the case of Ne $1s^{-1}$.

The KO mechanism described by Eq. (5) is the dominate mechanism for the direct DA process. Due to energy, angular momentum, and parity conversation, the continuum electrons from the primary SA processes coupling to the Ne^{2+} states should have specific energies and angular momenta [29], which are treated as incident electrons for the inelastic scattering in the KO mechanism. Besides, the emitted pairs of the Auger electrons that have the same total orbital angular momenta (in the LS scheme) and parities as the final Ne^{3+}

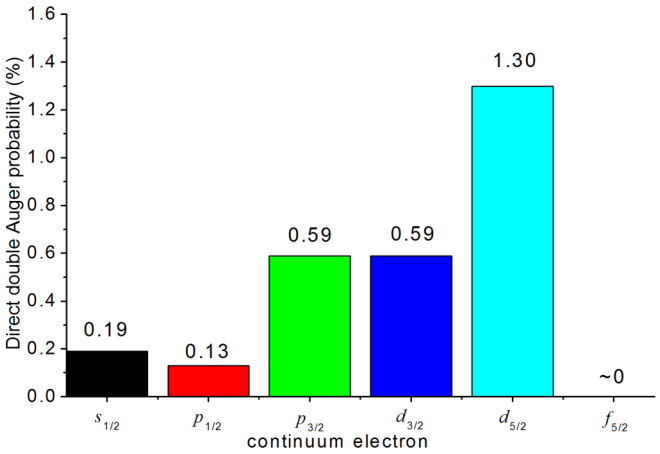

FIG. 1. The direct double Auger probabilities from the continuum electrons with specific angular momenta based on the knockout mechanism. The total direct double Auger probability for only the knockout mechanism included is 2.80% as listed in Table III.

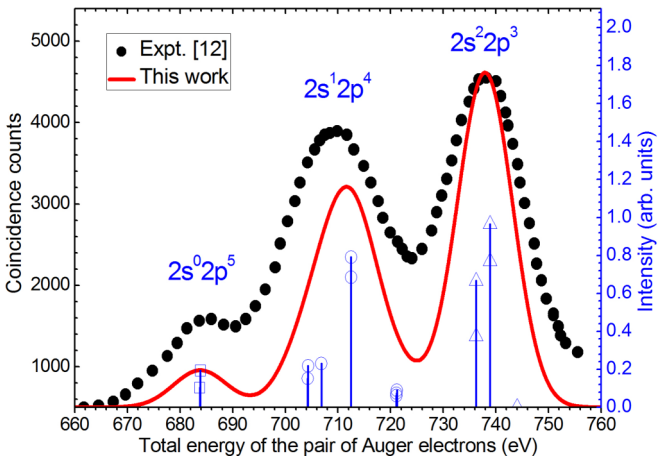

FIG. 2. Theoretical and experimental [12] spectra for the double Auger decays of Ne $1s^{-1}$. The solid vertical lines with symbols present relative intensities (with regard to the strongest transition that is normalized to one) corresponding to the levels of configurations $2s^2\,2p^3$ (open triangles), $2s^1\,2p^4$ (open circles), and $2s^0\,2p^5$ (open quadrangles) in the Ne^{3+} ion.

states, are permitted according to the restricted condition (9) in Ref. [33]. The direct DA probabilities from the continuum electrons with specific angular momenta are shown in Fig. 1 for the KO mechanism. The continuum electrons $d_{3/2}$ and $d_{5/2}$ emitted from the $KL_{23}L_{23}$ transition $1s^{-1} \rightarrow 2s^2\,2p^4\,{}^1D_2$ are responsible for the greatest DA probability of 1.89% of the Ne $1s^{-1}$ decay, which differs noticeably from the theoretical result by Kanngießer *et al.* [11] in which the $KL_{23}L_{23}$ transition produces the DA probability of only 0.66%. This may explain why their total DA probability of 3.05% [11] is much smaller than the experimental value of 5.97 ± 0.16% [11], whereas our total DA probability is 6.14% as shown in Table IV.

3. *The total double Auger process*

The calculated DA probabilities (in percentages) for the configurations $2s^2\,2p^3$, $2s2p^4$, and $2p^5$ of Ne^{3+} including the cascade and direct DA processes along with the available theoretical and experimental results are presented in Table IV. Our calculated cascade and direct DA probabilities are also in good agreement with the measurements [12] in Tables II and III, respectively, and then our total DA probability of 6.14% also agrees well with the experimental values (~6%) [9–11], which indicate that the current theoretical approaches and the main channels included adequately describe the DA processes of the Ne $1s^{-1}$ state. Our results as well as other theoretical works suggest that the most preferential configuration is $2s^2\,2p^3$ for the DA processes, which accounts for 52% of the total DA probability in the present paper. However, the recent experiment [12] showed that the most preferential channel is $2s2p^4$ rather than $2s^2\,2p^3$, which differs greatly from all theoretical results. In Fig. 2, we convolved the relative intensities (the strongest transition is normalized to one) of the Ne^{3+} levels with a Gaussian profile of 12-eV full width at half maximum (FWHM) (the estimated energy resolving power of the apparatus $E/\Delta E = 60$ in the energy region from 600 to 800 eV in Ref. [12]) and compared them with the experimental spectra [12] obtained by multielectron coincidence spectroscopy. From Fig. 2 the calculated spectra are found to reproduce the relative intensities of the main structures arising from the configurations $2s^2\,2p^3$, $2s2p^4$, and $2p^5$. However, the contributions from the configurations $2s2p^4$ and $2p^5$ are underestimated comparing to the experimental spectra.

As the average energy of the configuration $2s2p^4$ is greater by about 25 eV than that of $2s^2\,2p^3$ [34], the partial

TABLE IV. Probabilities (in percentages) of the double Auger decays of Ne $1s^{-1}$ along with the available theoretical and experimental values. The numbers in parentheses give the errors in the last significant digit for the experimental values.

	Theory				
Ne^{3+}	Ours	Ref. [15]	Ref. [11]	Ref. [14]	Expt.
$2s^2\,2p^3$	3.18	2.54	1.64	}2.50	2.50[a]
$2s2p^4$	2.62	2.14	1.18		2.90[a]
$2p^5$	0.34	0.71	0.19	1.50	0.50[a]
Total	6.14	5.39	3.05	4.00	5.97(16)[b], 5.40(70)[c], and 6.00[d]

[a]Reference [12].
[b]Reference [11].
[c]Reference [9].
[d]Reference [10].

TABLE V. Probabilities (in percentages) of the triple Auger decay of Ne $1s^{-1}$. The DDK and DDC indicate the contributions from the corresponding processes described as Eq. (8) in Sec. III C. The calculated triple Auger probabilities in column 4 with the inclusions of the DDK and DDC are compared with available theoretical [11] and experimental data [10–12].

	Theory				
Ne^{4+}	DDK	DDC	TA	Ref. [11]	Expt.
$2s^2\,2p^2$	0.026	0.034	0.060		0.18[a]
$2s2p^3$	0.061	0.004	0.065		0.18[a]
$2p^4$	0.022	∼0	0.022		0.03[a]
Total	0.109	0.038	0.147	0.05	0.38(5)[b] and 0.30[c]

[a]Reference [12].
[b]Reference [11].
[c]Reference [10].

DA probability of the configuration $2s2p^4$ may be affected by the missing high-n Rydberg-excited resonance states of Ne^{2+} that are limited in our paper due to the computational capacity. As discussed for the cascade process, using a larger scale of the configuration space to include more electron corrections may significantly affect the partial DA probabilities between the configurations. Therefore, refined theoretical calculations including more DA transition channels (namely, more high-n Rydberg-excited resonance states) and correlation contributions are sought to explain this unexpected difference. Meanwhile, we also look forward to forthcoming experiments with higher resolution that allow resolving the individual fine-structure levels of the final Ne^{3+} ion to offer detailed experimental results to test the theory further.

C. Triple Auger decay

The Ne $1s^{-1}$ state that lies above the ground configuration $1s^2\,2s^2\,2p^2$ of Ne^{4+} can decay with a three-electron emission as observed in experiments [10,11]. Similar to DA analyses, the TA processes could be decomposed into a sequence of multistep processes with the KO and cascade mechanisms. Here, we safely can assume that the contribution of the SO mechanism could be neglected after the DA process since the contribution of the SO to the direct DA decay is much smaller than that of the KO mechanism as shown in Table III. This is also true for the direct DA process of C $1s^{-1}$ [21]. Therefore, the TA processes described by Eq. (3) could be considered by the four categories denoted as CDC, CDK, DDC, and DDK as follows:

$$\begin{aligned}
&\text{(a)}\ \mathrm{Ne}1s^{-1}(\alpha) \xrightarrow{\text{cascade DA}} \mathrm{Ne}^{3+}(\gamma)^* + e^-(\varepsilon_1 l_1) + e^-(\varepsilon_2 l_2) \xrightarrow{\text{cascade}} \mathrm{Ne}^{4+}(\delta) + e^-(\varepsilon_1 l_1) + e^-(\varepsilon_2 l_2) + e^-(\varepsilon_3 l_3)(\text{CDC});\\
&\text{(b)}\ \mathrm{Ne}1s^{-1}(\alpha) \xrightarrow{\text{cascade DA}} \mathrm{Ne}^{3+}(\gamma) + e^-(\varepsilon_1 l_1) + e^-(\varepsilon_2 l_2) \xrightarrow{\text{knockout}} \mathrm{Ne}^{4+}(\delta) + e^-(\varepsilon_1 l_1) + e^-(\varepsilon_2 l_2) + e^-(\varepsilon_3 l_3)(\text{CDK});\\
&\text{(c)}\ \mathrm{Ne}1s^{-1}(\alpha) \xrightarrow{\text{direct DA}} \mathrm{Ne}^{3+}(\gamma)^* + e^-(\varepsilon_1 l_1) + e^-(\varepsilon_2 l_2) \xrightarrow{\text{cascade}} \mathrm{Ne}^{4+}(\delta) + e^-(\varepsilon_1 l_1) + e^-(\varepsilon_2 l_2) + e^-(\varepsilon_3 l_3)(\text{DDC});\\
&\text{(d)}\ \mathrm{Ne}1s^{-1}(\alpha) \xrightarrow{\text{direct DA}} \mathrm{Ne}^{3+}(\gamma) + e^-(\varepsilon_1 l_1) + e^-(\varepsilon_2 l_2) \xrightarrow{\text{knockout}} \mathrm{Ne}^{4+}(\delta) + e^-(\varepsilon_1 l_1) + e^-(\varepsilon_2 l_2) + e^-(\varepsilon_3 l_3)(\text{DDK}),
\end{aligned} \tag{8}$$

where the states with asterisks represent the resonance states of Ne^{3+} that lie energetically above the Ne^{4+} threshold, which will autoionize further to the Ne^{4+} states. In the case of the CDC, this is a fully sequential cascade process since the intermediate resonance states of the Ne^{2+} and Ne^{3+} ions are created in the whole TA process. The CDC probability is estimated to be only 0.005% with considerations of the intermediate resonance states ($n < 5$, $l < 3$) of Ne^{2+} and Ne^{3+}. These resonance states are limited in the calculations, but the contributions of the higher nl should be even smaller. In the CDK processes, two electrons are emitted sequentially via a primary cascade DA decay, and then the second electron could ionize a bound electron of Ne^{3+} by inelastic scattering (knockout) and lead to the Ne^{4+} states. Due to the energy conservation, the energy range of the second Auger electron from the cascade DA processes is about 0–40 eV and was observed in the experiment [12]. However, such an Auger electron in this energy range is insufficient to eject a bound electron in the Ne^{3+} ion because the ionization potential of Ne^{3+} is 97.19 eV [34]. Therefore, the CDK processes are neglected in this paper.

We mainly focus on cases (3) and (4), namely, the DDC and DDK processes, respectively. In the DDC process, the resonances states of Ne^{3+} are created via a direct DA process, and these resonances states autoionize further to the Ne^{4+} states. The DDC probabilities are presented in Table V with the most preferential configuration being $2s^2 2p^2$ that account for almost 90% of the DDC processes. For the DDK process, the three-electron emission is decomposed into a simultaneous two-electron emission via a direct DA process and a subsequent inelastic scattering process (knockout) to ionize the third bound electron of the Ne^{3+} ion. The triple Auger rate of the DDK process can be expressed by

$$\begin{aligned}
A^3_{\alpha\gamma\delta} &= A^2_{\alpha\gamma}\int_0^{E_{\max}/2} \rho_{\alpha\gamma}(\varepsilon)\big[\Omega_{\gamma\delta}(\varepsilon) + \Omega_{\gamma\delta}(E_{\max}-\varepsilon)\big]d\varepsilon\\
&= A^2_{\alpha\gamma}\int_0^{E_{\max}} \rho_{\alpha\gamma}(\varepsilon)\Omega_{\gamma\delta}(\varepsilon)d\varepsilon,
\end{aligned} \tag{9}$$

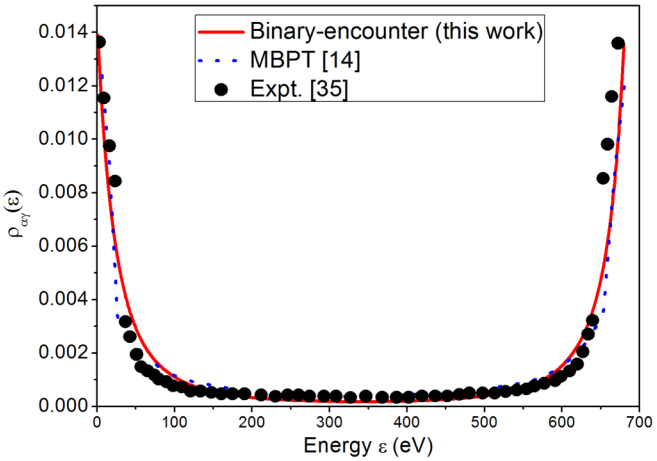

FIG. 3. Normalized distribution of the energy of the Auger electrons for the direct double Auger decay $1s^{-1}\,{}^2S \rightarrow 2p^5\,{}^2P$. The present binary-encounter results (the red solid line) are compared with the values from many-body perturbation theory (the blue dotted line) [14] and experiment (the solid circles) [35].

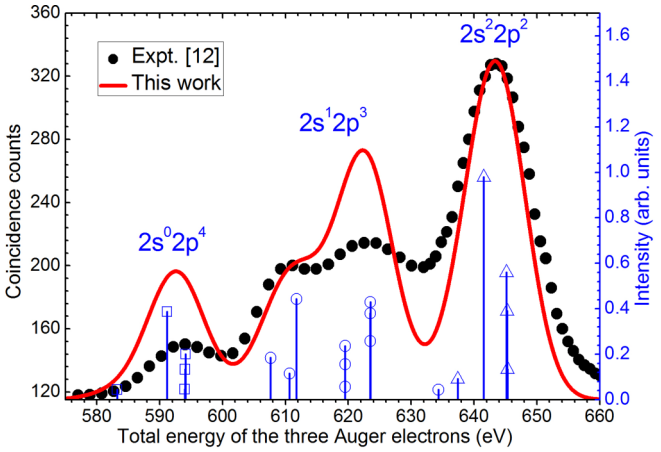

FIG. 4. Theoretical and experimental [12] spectra for the triple Auger decays of Ne $1s^{-1}$. The solid vertical lines with symbols present relative intensities (with regard to the strongest transition that is normalized to one) corresponding to the levels of configurations $2s^2\,2p^2$ (open triangles), $2s^1\,2p^3$ (open circles), and $2s^0\,2p^4$ (open quadrangles) in the Ne^{4+} ion.

where $A^2_{\alpha\gamma}$ is the direct DA rate from the initial-state Ne $1s^{-1}$ to the intermediate Ne^{3+} state in which it instantaneously emits two continuum electrons sharing the continuously distributed energies of $E_{\max} = E_\alpha - E_\beta$. E_α and E_β are the energies of the initial-state Ne $1s^{-1}$ and the final state of Ne^{3+}, respectively. $\Omega_{\gamma\delta}(\varepsilon)$ and $\Omega_{\gamma\delta}(E_{\max} - \varepsilon)$ are the collision strength of inelastic scattering off a bound electron of Ne^{3+} by the two intermediate Auger electrons. One of the intermediate Auger electrons carries away almost all the energies, based on the fact that each of the ejected electrons has a kinetic energy between 0 and $E_{\max}$ with the symmetrical U-shaped energy distribution in the direct DA process [12,14,35]. $\rho_{\alpha\gamma}(\varepsilon)$ is the normalized distribution of the total energy between two continuum electrons that was obtained approximately by using a normalized single energy differential cross section according to the binary-encounter model [36]. In Fig. 3, we illustrate the validity of the binary-encounter model and compare the energy distribution of the intermediate Auger electrons for the direct DA decay $1s^{-1} \rightarrow 2s^{-2}2p^{-1}\,{}^2P$ along with the theoretical values by MBPT [14] and experimental values [35]. It is found that the binary-encounter model could properly describe the energy distribution of the Auger electron for the direct DA process of Ne $1s^{-1}$, which is also true for the case of C^+ $1s^{-1}$ [21].

The TA probabilities for the DDC and DDK processes are presented in Table V. The total and partial TA probabilities decaying to the dominant configurations $2s^2\,2p^2$, $2s2p^3$, and $2p^4$ of Ne^{4+} along with the available theoretical [11] and experimental values [10–12] also are presented. The DDK processes are dominant, which account for 74% of the TA decays. The ratio of the partial DDK probabilities is $(2s^2\,2p^2) : (2s2p^3) : (2p^4) = 1.2 : 2.8 : 1$, which suggests that the most preferential configuration is $2s2p^3$. The ratio of the partial TA probabilities including the DDC and DDK is $(2s^2\,2p^2) : (2s2p^3) : (2p^4) = 2.7 : 2.9 : 1$, which is reasonably consistent with the measurement of 6.7:6.8:1 [12], as the absolute value for $2p^4$ is rather small. Finally, the calculated total TA probability of 0.152% including the CDC, DDC, and DDK processes is three times greater than the earlier theoretical work of only 0.05% [11] but is still half the experimental value [10,11]. The TA spectra convolved with a Gaussian profile of 10-eV FWHM is compared with the experimental spectra [12] in Fig. 4, and all main structures from the configurations $2s^2\,2p^2$, $2s2p^3$, and $2p^4$ are present. For the TA decay as the high-order process, we should mention that the systematic absolute uncertainty could be large due to extremely weak coincidence counts for detecting the yields produced by the TA decays, e.g., recently Müller *et al.* [37] reported an estimation of the uncertainty of ±50% for the observation of the direct TA processes in the C^+ ion.

IV. CONCLUSION

In this paper we presented the theoretical study of multiple Auger decays including double and triple Auger processes for neon with a hole in the 1*s* shell. The transition amplitudes of multiple Auger processes where more than two single-electron orbits are changing are evaluated beyond the independent-particle model by using multistep approaches derived from many-body perturbation theory, namely, the cascade, knockout, and shakeoff mechanisms. The present results show that the orbital sets constructed by the inclusion of several configurations $1s^2\,2s^2\,2p^4$, $1s^2\,2s2p^5$, $1s^2\,2p^6$, and $1s^2\,2s^2\,2p^3 3p$ of Ne^{2+} increase the cascade double Auger probability to about 3%, whereas inclusion of $1s^2\,2s^2\,2p^4$, $1s^2\,2s2p^5$, and $1s^2\,2p^6$ produce about 1%. The direct double Auger probabilities are 2.80% and 0.37% by the knockout and shakeoff mechanisms, respectively, which indicate that the knockout mechanism is dominant. The cascade and direct double Auger probabilities as well as the resulting total double Auger decay probability of 6.14% are consistent with the available experimental data. As have been discussed for the double Auger processes, the complex triple Auger processes can be decomposed into four categories based on the multistep approaches and two of which are focused mainly

on: $1s^{-1}(\alpha) \xrightarrow{\text{direct DA}} \mathrm{Ne}^{3+}(\gamma)^* + e^-(\varepsilon_1 l_1) + e^-(\varepsilon_2 l_2) \xrightarrow{\text{cascade}} \mathrm{Ne}^{4+}(\delta) + e^-(\varepsilon_1 l_1) + e^-(\varepsilon_2 l_2) + e^-(\varepsilon_3 l_3)$; $1s^{-1}(\alpha) \xrightarrow{\text{direct DA}} \mathrm{Ne}^{3+}(\gamma) + e^-(\varepsilon_1 l_1) + e^-(\varepsilon_2 l_2) \xrightarrow{\text{knockout}} \mathrm{Ne}^{4+}(\delta) + e^-(\varepsilon_1 l_1) + e^-(\varepsilon_2 l_2) + e^-(\varepsilon_3 l_3)$. The present total triple Auger probability of 0.152% is three times greater than the earlier theoretical work of only 0.05% but is still half the available experimental values [10,11], and further experiments are expected.

ACKNOWLEDGMENTS

One of the authors, Yizhi Qu, would like to thank Professor Y. Ralchenko for the helpful discussions during his stay at NIST. This work was supported by the National Key Research and Development Program of China under Grant No. 2017YFA0402300, the National Natural Science Foundation of China (Grants No. 11774344 and No. 11474033), and the NSAF (Grant No. U1330117).

[1] N. Stolterfoht, C. C. Havener, R. A. Phaneuf, J. K. Swenson, S. M. Shafroth, and F. W. Meyer, Phys. Rev. Lett. **57**, 74 (1986).
[2] F. Penent, J. Palaudoux, P. Lablanquie, L. Andric, R. Feifel, and J. H. D. Eland, Phys. Rev. Lett. **95**, 083002 (2005).
[3] B. Denne, E. Hinnov, J. Ramette, and B. Saoutic, Phys. Rev. A **40**, 1488 (1989).
[4] J. Y. Dai, Y. Hou, and J. M. Yuan, Phys. Rev. Lett. **104**, 245001 (2010).
[5] V. Jonauskas, P. Bogdanovich, F. P. Keenan, R. Kielius, M. E. Foord, R. F. Heeter, S. J. Rose, G. J. Ferland, and P. H. Norrington, Astron. Astrophys. **455**, 1157 (2006).
[6] T. R. Kallman and P. Palmeri, Rev. Mod. Phys. **79**, 79 (2007).
[7] B. Lin, H. G. Berry, T. Shibata, A. E. Livingston, H.-P. Garnir, T. Bastin, J. Désequelles, and I. Savukov, Phys. Rev. A **67**, 062507 (2003).
[8] A. Lapierre and É. J. Knystautas, J. Phys. B: At., Mol. Opt. Phys. **33**, 2245 (2000).
[9] T. A. Carlson and M. O. Krause, Phys. Rev. Lett. **14**, 390 (1965).
[10] S. Norio and H. S. Isao, Phys. Scr. **49**, 80 (1994).
[11] B. Kanngießer, M. Jainz, S. Brünken, W. Benten, C. Gerth, K. Godehusen, K. Tiedtke, P. van Kampen, A. Tutay, P. Zimmermann, V. F. Demekhin, and A. G. Kochur, Phys. Rev. A **62**, 014702 (2000).
[12] Y. Hikosaka, T. Kaneyasu, P. Lablanquie, F. Penent, E. Shigemasa, and K. Ito, Phys. Rev. A **92**, 033413 (2015).
[13] A. G. Kochur, V. L. Sukhorukov, A. J. Dudenko, and P. V. Demekhin, J. Phys. B: At., Mol. Opt. Phys. **28**, 387 (1995).
[14] M. Y. Amusia, I. S. Lee, and V. A. Kilin, Phys. Rev. A **45**, 4576 (1992).
[15] A. G. Kochur, V. L. Sukhorukov, and V. F. Demekhin, J. Electron Spectrosc. Relat. Phenom. **137–140**, 325 (2004).
[16] M. F. Gu, Can. J. Phys. **86**, 675 (2008).
[17] S. Fritzsche, Comput. Phys. Commun. **183**, 1525 (2012).
[18] J. Zeng, P. Liu, W. Xiang, and J. Yuan, Phys. Rev. A **87**, 033419 (2013).
[19] T. Pattard and J. Burgdörfer, Phys. Rev. A **63**, 020701(R) (2001).
[20] J. L. Zeng, P. F. Liu, W. J. Xiang, and J. M. Yuan, J. Phys. B: At., Mol. Opt. Phys. **46**, 215002 (2013).
[21] F. Zhou, Y. Ma, and Y. Qu, Phys. Rev. A **93**, 060501(R) (2016).
[22] T. Schneider, P. L. Chocian, and J. M. Rost, Phys. Rev. Lett. **89**, 073002 (2002).
[23] S. Fritzsche, B. Fricke, and W.-D. Sepp, Phys. Rev. A **45**, 1465 (1992).
[24] S. Fritzsche, J. Nikkinen, S. -M. Huttula, H. Aksela, M. Huttula, and S. Aksela, Phys. Rev. A **75**, 012501 (2007).
[25] F. von Busch, U. Kuetgens, J. Doppelfeld, and S. Fritzsche, Phys. Rev. A **59**, 2030 (1999).
[26] P. Jönsson, X. He, C. Froese Fischer, and I. P. Grant, Comput. Phys. Commun. **177**, 597 (2007).
[27] S. Fritzsche, C. F. Fischer, and G. Gaigalas, Comput. Phys. Commun. **148**, 103 (2002).
[28] H. P. Kelly, Phys. Rev. A **11**, 556 (1975).
[29] J. Tulkki, T. Åberg, A. Mäntykenttä, and H. Aksela, Phys. Rev. A **46**, 1357 (1992).
[30] V. G. Yarzhemsky and A. Sgamellotti, J. Electron Spectrosc. Relat. Phenom. **125**, 13 (2002).
[31] A. Albiez, M. Thoma, W. Weber, and W. Mehlhorn, Z. Phys. D: At., Mol. Clusters **16**, 97 (1990).
[32] S. Svensson, N. Mårtensson, E. Basilier, P. A. Malmquist, U. Gelius, and K. Siegbahn, Phys. Scr. **14**, 141 (1976).
[33] A. N. Grum-Grzhimailo and N. M. Kabachnik, J. Phys. B: At., Mol. Opt. Phys. **37**, 1879 (2004).
[34] A. Kramida, Y. Ralchenko, J. Reader, and the NIST ASD Team (2015), NIST Atomic Spectra Database (version 5.3) (online). Available: http://physics.nist.gov/asd (2017).
[35] J. Viefhaus, A. N. Grum-Grzhimailo, N. M. Kabachnik, and U. Becker, J. Electron Spectrosc. Relat. Phenom. **141**, 121 (2004).
[36] Y.-K. Kim and M. E. Rudd, Phys. Rev. A **50**, 3954 (1994).
[37] A. Müller, A. Borovik, Jr., T. Buhr, J. Hellhund, K. Holste, A. L. D. Kilcoyne, S. Klumpp, M. Martins, S. Ricz, J. Viefhaus, and S. Schippers, Phys. Rev. Lett. **114**, 013002 (2015).